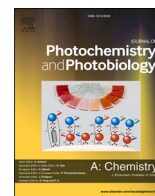




Contents lists available at ScienceDirect

## Journal of Photochemistry &amp; Photobiology, A: Chemistry

journal homepage: [www.elsevier.com/locate/jphotochem](http://www.elsevier.com/locate/jphotochem)

# Photoprocesses in *bis*(15-crown-5)-1,3-distyrylbenzene and its complexes with metal perchlorates

Levon S. Atabekyan<sup>a,\*</sup>, Vitaly G. Avakyan<sup>a</sup>, Alexander K. Chibisov<sup>a</sup>, Vyacheslav N. Nuriev<sup>a,b</sup>, Alexey V. Medvedko<sup>a,b</sup>, Alexander V. Koshkin<sup>a</sup>, Sergey P. Gromov<sup>a,b</sup>

<sup>a</sup> Photochemistry Center of RAS, FSRC "Crystallography and Photonics", Russian Academy of Sciences, Novatorov Str. 7A-1, Moscow, 119421, Russian Federation

<sup>b</sup> Department of Chemistry, M. V. Lomonosov Moscow State University, Leninskie Gory 1-3, Moscow, 119991, Russian Federation

## ARTICLE INFO

## Keywords:

1,3-distyrylbenzene  
Laser pulse photolysis  
Complex formation  
*Trans-cis*-isomerization  
Triplet state  
[2 + 2]-photocycloaddition

## ABSTRACT

Photoprocesses in *bis*(15-crown-5)-1,3-distyrylbenzene (DSB) and its complexes with barium and lead perchlorates were studied in MeCN by absorption, luminescence, and laser kinetic spectroscopy. The triplet DSB molecules are involved in the degradation of electronic excitation energy, together with fluorescence processes. The most efficient intersystem crossing accompanied by a decrease in the DSB fluorescence quantum yield, occurs for the lead perchlorate complex. Using quantum chemistry methods (DFT and TDDFT), the geometry, structure, and transition energies to the S<sub>1</sub> state were calculated for *trans*- and *cis*-isomers of DSB in the gas phase and with allowance for the solvent and for 1:1 and 2:2 DSB complexes with barium cation in the ground and excited states. The orbital structures of the 2:2 complexes were calculated by *ab initio* method, and conclusions were drawn about the possibility of [2 + 2]- photocycloaddition reaction.

## 1. Introduction

Crown-containing unsaturated compounds, in particular, *bis*-crown-containing distyrylbenzenes (DSB) are of considerable interest as photoactive components of supramolecular systems [1]. Molecules of these compounds are able to form supramolecular assemblies when complexed with metal cations [2]. Distyrylbenzenes are characterized by relatively high quantum yields of fluorescence [3,4]. The presence of two C=C bonds in these molecules brings about additional possibilities for photoswitching [5,6], which makes the compounds promising for the development of light-sensitive materials for data recording. This feature and some other properties make distyrylbenzenes attractive molecules for the design of photoactive materials: organic light-emitting diodes, materials for solar batteries, nonlinear-optical materials, and chemical sensors [7–12].

Previously, we studied the photonics of *bis*(15-crown-5)-1,4-distyrylbenzene (*II*) and its complexes with metal cations [13] and demonstrated that the complex formation of *II* with barium and lead perchlorates is accompanied by transfer of the molecule to the triplet state. This is accompanied by a considerable decrease in the fluorescence quantum yield. The calculations also showed that *II* can form 2:2 *bis*-sandwich complexes with barium perchlorate (Scheme 1).

This study addresses *bis*(15-crown-5)-1,3-distyrylbenzene (*I*) and the complexes it forms with barium and lead perchlorates. Photo-transformations of dye *I* and its metal complexes were studied by laser kinetic spectroscopy. Our goal was to establish the existence of intermediate products of photoreactions, in particular, the triplet state of *I* and its complexes and to compare the results with experimental data obtained for *II*. In addition to experimental studies, quantum chemical calculations were carried out.

## 2. Experimental procedure

### 2.1. Materials and methods

*Bis*(15-crown-5)-1,3-distyrylbenzene was synthesized according to the procedure described in reference [14]. The synthesis protocol and characterization data (<sup>1</sup>H NMR, <sup>13</sup>C NMR, mass spectrum and elemental analysis) are given therein.

The absorption spectra of dye *I* were obtained on an Agilent 8453 spectrophotometer. Luminescence spectra were recorded on a Varian Eclipse spectrofluorimeter. The difference absorption spectra of the photoproducts and the reaction kinetics were measured on a nanosecond laser photolysis setup [15]. Irradiation was performed with the third

\* Corresponding author.

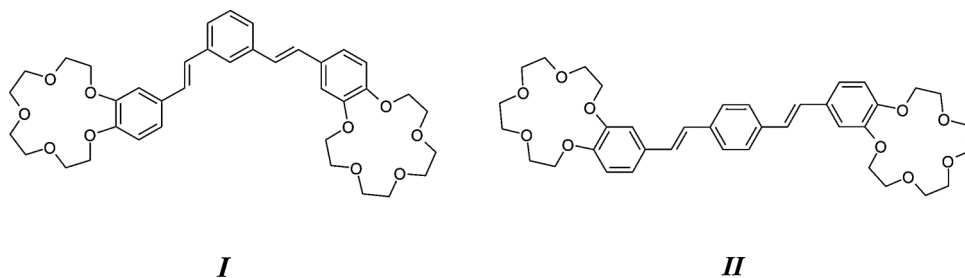
E-mail address: [levat51@mail.ru](mailto:levat51@mail.ru) (L.S. Atabekyan).

<https://doi.org/10.1016/j.jphotochem.2021.113293>

Received 18 January 2021; Received in revised form 9 April 2021; Accepted 10 April 2021

Available online 14 April 2021

1010-6030/© 2021 Elsevier B.V. All rights reserved.



**Scheme 1.** Structures of bis(15-crown-5)-1,3-distyrylbenzene (**I**) and bis(15-crown-5)-1,4-distyrylbenzene (**II**).

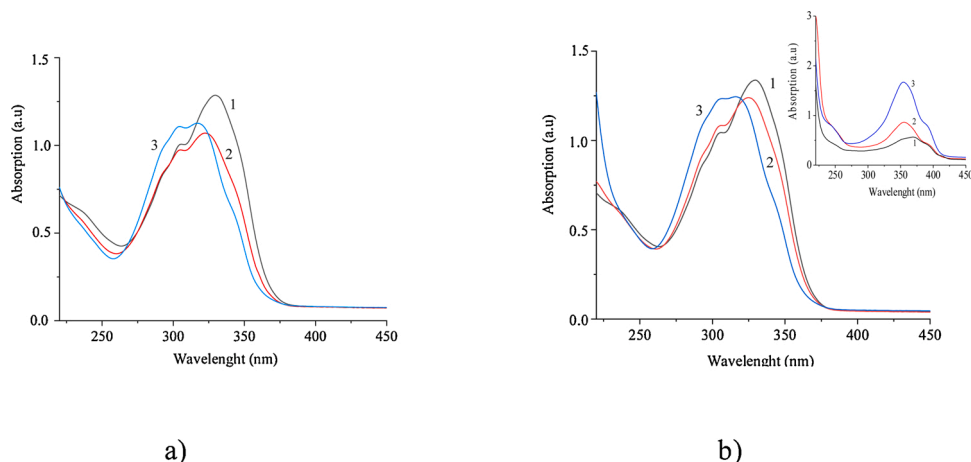


**Fig. 1.** Absorption spectra of **I** in the absence (1) and in presence (2, 3) of  $\text{Ba}(\text{ClO}_4)_2$  (a) and  $\text{Pb}(\text{ClO}_4)_2$  (b). Concentrations: **I**,  $2 \times 10^{-5}$ ; metal salts,  $1 \times 10^{-5}$  (2),  $2 \times 10^{-4}$  (3) mol/L. The inset shows the absorption spectra of **II** in the absence (1) and in presence of  $\text{Pb}(\text{ClO}_4)_2$  (2) and  $\text{Ba}(\text{ClO}_4)_2$  (3). Concentrations: **II**,  $1 \times 10^{-5}$ ; metal salts,  $3 \times 10^{-4}$  mol/L.

harmonic of a Solar laser ( $\lambda = 355$  nm). The dissolved oxygen was removed by bubbling argon through the solution. The stationary irradiation of dye solutions was performed using a DKSSh (Hg-150 lamp) with a UFS-2 filter. 9,10-Diphenylanthracene (the quantum yield is 0.92 in ethanol [16]) was used as the standard for measuring fluorescence quantum yields. The accuracy of quantum yield determination was 10 %. Potassium perchlorate (monohydrate), lead perchlorate (trihydrate), and barium perchlorate (Merck) were used as received. The measurements were carried out in MeCN (special purity grade, brand 0, Cryochrome) at room temperature.

## 2.2. Calculation procedure

Quantum chemical calculations were performed by *ab initio* and DFT methods. Geometry optimization for *trans*- and *cis*-isomers of **I** in the gas phase and in the presence of a solvent and for barium complexes of **I** —  $\text{I}\cdot\text{Ba}^{2+}$  and double-decker complex  $2\text{I}\cdot 2\text{Ba}^{2+}$  — in the ground  $\text{S}_0$  state was carried out by the ORCA software [17] in the def2-SVP basis set [18] with the PBE0 functional [19] with inclusion of the dispersion correction D3 [20]. The transfer energies and structures of *trans*- and *cis*-**I** in the excited  $\text{S}_1$  state were calculated at the TDDFT/PBE0/def2-VP level for the gas phase and in terms of the polarized continuum model (PCM) to account for solvent effects. Earlier the calculations performed with this functional including 20–25 % HF exchange were shown to result in qualitative agreement with the structure and energetics of excited states obtained by XMCQDPT2/CASSCF calculations [21]. The structures of **I** and complexes  $\text{I}\cdot\text{Ba}^{2+}$  and  $2\text{I}\cdot 2\text{Ba}^{2+}$  in the electronically excited  $\text{S}_1$  state were optimized by the TDDFT/PBE0/def2-VP method. The orbital structures and formation energies of  $\text{I}\cdot\text{Ba}^{2+}$  and  $2\text{I}\cdot 2\text{Ba}^{2+}$  in the excited state were found, for higher reliability, by *ab initio* calculations in the def2-TZVP three-exponential basis set with and without the inclusion of the dispersion correction D3. The *ab initio* calculation level is fully designated as ground  $\text{S}_0$  state was found by subtracting twice the energy of the fully optimized complexes  $E_{\text{total}}(\text{I}\cdot\text{Ba}^{2+})$  from the optimized energy  $E_{\text{total}}(2\text{I}\cdot 2\text{Ba}^{2+})$ . The complex formation energy in the excited  $\text{S}_1$  state,  $\Delta E_{\text{compl}}^*$ , was determined by subtracting the sum of  $E_{\text{total}}(\text{I}\cdot\text{Ba}^{2+})$  and  $E_{\text{total}}^*(\text{I}\cdot\text{Ba}^{2+})$  from the energy of the fully optimized complex  $E_{\text{total}}^*(2\text{I}\cdot 2\text{Ba}^{2+})$ .

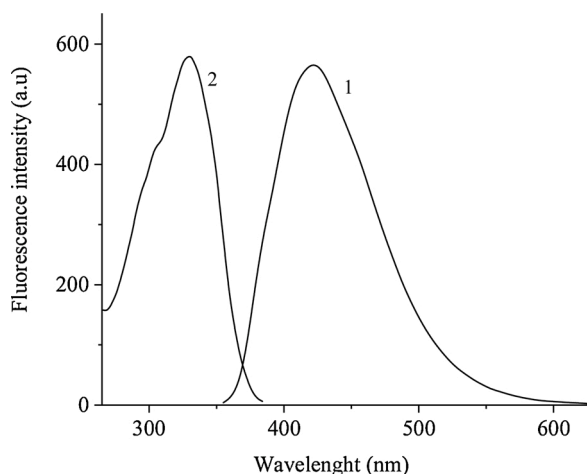


**Fig. 2.** Fluorescence **I** (1) and fluorescence excitation (2) spectra. Concentration of **I**:  $2.5 \times 10^{-6}$  mol/L.  $\lambda_{\text{excit}} = 330$  nm (1),  $\lambda_{\text{fl}} = 420$  nm (2).

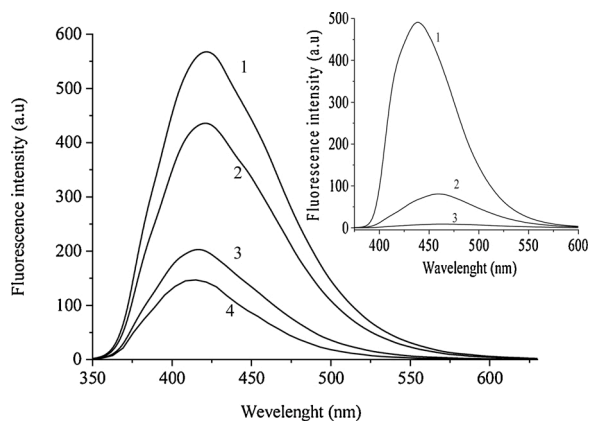


**Fig. 3.** Fluorescence spectra of *I* in the absence (1) and in presence (2–4) of Ba(ClO<sub>4</sub>)<sub>2</sub>. Concentrations: *I*,  $2.5 \times 10^{-6}$ ; Ba(ClO<sub>4</sub>)<sub>2</sub>,  $1.25 \times 10^{-6}$  (2),  $2.5 \times 10^{-6}$  (3), and  $5 \times 10^{-6}$  (4) mol/L. The inset shows the fluorescence spectra of *II* in the absence (1) and in presence of Ba(ClO<sub>4</sub>)<sub>2</sub> (2) and Pb(ClO<sub>4</sub>)<sub>2</sub> (3). Concentrations: *II*,  $5 \times 10^{-6}$ ; metal salts,  $6 \times 10^{-5}$  mol/L.

**Table 1**

Quantum yields ( $\phi$ ) and fluorescence maxima of *I* and complexes of *I* with potassium, barium, and lead cations. Concentrations: *I*,  $5 \times 10^{-6}$ ; metal perchlorates,  $1 \times 10^{-5}$  mol/L.

Compound	<i>I</i>	<i>I</i> + Ba <sup>2+</sup>	<i>I</i> + Pb <sup>2+</sup>	<i>I</i> + K <sup>+</sup>
$\phi$	0.47	0.46	0.05	0.48
$\lambda_{\max}$ , nm	423	416	416	423

### 3. Experimental results and discussion

#### 3.1. Absorption and fluorescence spectra

Fig. 1 shows the absorption spectrum of *I* in the absence (1) and in presence (2, 3) of metal perchlorates. The spectrum of *I* is poorly resolved and consists of a band with  $\lambda_{\max} = 330$  nm and two shoulders with maxima at 305 and 350 nm.

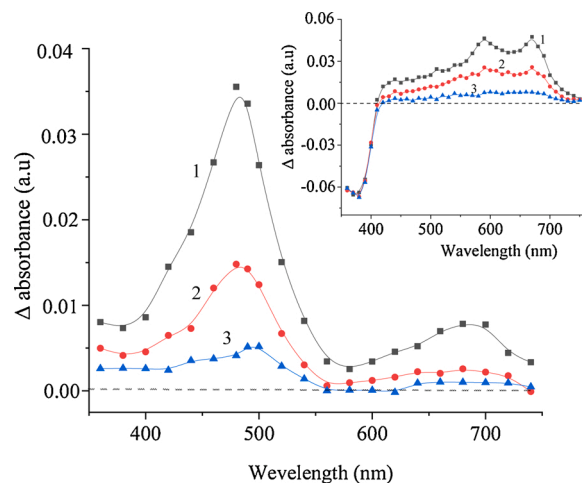
In the presence of metal perchlorates, the spectrum of *I* shows a blue shift of absorption maximum, with the maximum shifted for 5 and 20 nm depending on the metal salt concentration. The concentration dependence of the spectra indicates that complexes of different composition may exist. The inset in the Figure presents the absorption spectra of *II* in the presence of barium and lead cations. 1,3-Distyrylbenzenes absorb at shorter wavelengths ( $\lambda_{\max} = 329\text{--}331$  nm) than 1,4-distyrylbenzenes ( $\lambda_{\max} = 370\text{--}372$  nm), which is due to efficient  $\pi$ -conjugation over the whole chromophore in the case of 1,4-disubstitution. In 1,3-disubstituted benzenes, the conjugation is substantially disrupted or absent; therefore, their absorption spectra can be approximately considered the sum of the spectra of two independent stilbene moieties.

Fig. 2 shows the fluorescence and fluorescence excitation spectra of *I*.

The fluorescence excitation spectrum almost coincides with the absorption spectrum of *I*. A considerable Stokes shift (90 nm) is observed between the fluorescence and fluorescence excitation maxima. Fluorescence spectra of *I* in the absence (1) and in presence of Ba(ClO<sub>4</sub>)<sub>2</sub> (2–4) are shown in Fig. 3.

In the presence of barium cations, fluorescence intensity slightly decreases, while in the presence of lead cations, it considerably decreases (by a factor of 10), and the fluorescence maxima slightly shift to shorter wavelengths (by 7 nm). Table 1 summarizes the absorption maxima and fluorescence quantum yields of *I* and metal cation complexes of *I*.

It is noteworthy that the slight differences between the absorption and fluorescence spectra of free compound *I* and the complexes considerably complicated determination of the corresponding stability



**Fig. 4.** Photoinduced absorption difference spectra measured upon laser irradiation of an oxygen-free solution of *I*. The spectra were measured at 2 (1), 75 (2), and 425 (3)  $\mu$ s after the laser pulse. The inset shows the absorption difference spectra recorded upon laser irradiation of an oxygen-free solution of *II* within 2 (1), 75 (2), and 425 (3)  $\mu$ s after the laser pulse.

constants of the complexes.

#### 3.2. Kinetic spectroscopy

Fig. 4 shows the difference spectra of photoinduced absorption measured upon laser irradiation of an oxygen-free solution of *I* within 2, 75, and 425  $\mu$ s after the end of the laser pulse. The difference spectra show the bands of increasing absorption at 400–550 nm and 600–750 nm. For comparison, the inset shows similar difference spectra measured at the same time points for compound *II*.

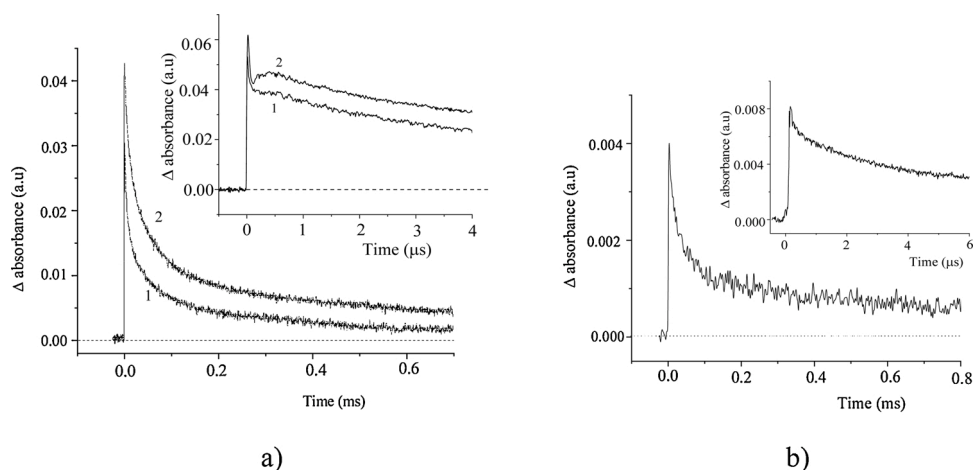
As can be seen from the Figure, the difference spectrum measured upon laser excitation of an oxygen-free solution of *II* differs considerably from the corresponding spectrum of *I*. In the case of *II*, the absorbance in the major absorption region decreases and two absorption bands appear at  $\lambda_{\max} = 600$  and 700 nm.

Fig. 5 shows the kinetic curves for the photoinduced change in the absorbance measured at the band maxima of the difference spectrum:  $\lambda_{\max} = 480$  nm (a) and 700 nm (b).

The dependence of the kinetics of decrease in the photoinduced absorption on the air oxygen concentration in the solution attests to either T-T absorption or transformation of radical reaction products. The kinetics for the change in the absorbance at a millisecond time scale is biexponential, with the observed rate constants being  $6 \times 10^4$  s<sup>-1</sup> and  $8 \times 10^3$  s<sup>-1</sup> at 480 nm for oxygen-free solutions. The presence of air oxygen mainly affects the change in the absorbance ( $\Delta A$ ) at 480 nm. No effect of air oxygen on the absorbance or the kinetics of absorbance change at 680 nm is observed. The effect of air oxygen in the microsecond time scale is illustrated in the inset of Fig. 5a. Despite the similarity of the rate constants for the transformation of photoreaction intermediates at  $\lambda_{\max} = 480$  and 680 nm, different photoproducts are presumably formed at these wavelengths, as indicated by the kinetic curves depicted in the insets of Fig. 5a and b. The observed photoconversion is not related to the *trans-cis*-isomerization, since according to the quantum mechanical calculation (see below), the absorption band of the *cis*-isomer occurs at shorter wavelengths than the *trans*-isomer band.

In order to confirm participation of the triplet state in the photoconversions of *I*, we measured the spectrum and the kinetics for the photoinduced change in the absorbance of *I* in the presence of benzophenone, as a sensitizer taken in excess with respect to *I*. The results are depicted in Fig. 6.

Qualitatively, the difference spectrum and the kinetics for the



**Fig. 5.** Kinetic curves for the photoinduced change in the absorbance of *I* for air-saturated (1) and oxygen-free (2) solutions at  $\lambda = 480$  nm (a) and for oxygen-free solution at 680 nm (b). The insets show the kinetic curves for the change in absorbance on an enlarged time scale.

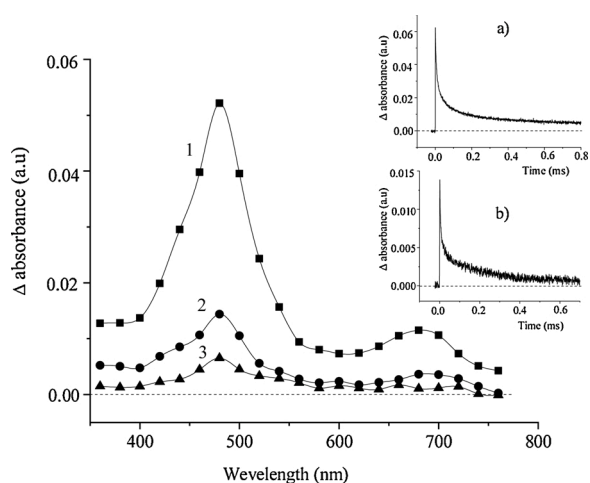


**Fig. 6.** Photoinduced absorption difference spectra of an oxygen-free solution of *I* in the presence of benzophenone, measured at 2 (1), 75 (2), and 425 (3)  $\mu$ s after the laser pulse. Concentrations: *I*,  $2 \times 10^{-5}$ ; benzophenone,  $2.3 \times 10^{-4}$  mol/L. The insets show the kinetic curves for the photoinduced change in the absorbance at  $\lambda = 480$  (a) and 680 (b) nm.

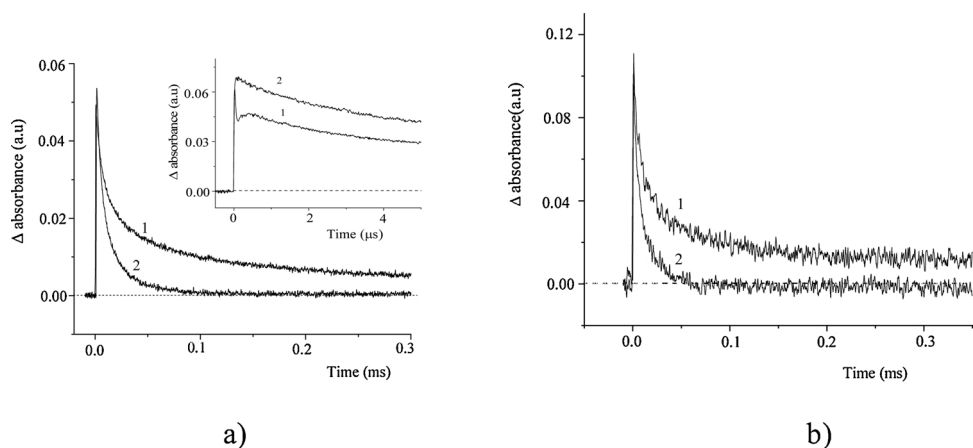


**Fig. 7.** Kinetic curves for the change in the photoinduced absorbance of *I* in the absence (1) and in presence (2) of ascorbic acid.  $\lambda = 480$  nm (a) and 680 nm (b). Concentrations: *I*,  $2 \times 10^{-5}$ ; ascorbic acid,  $2 \times 10^{-4}$  mol/L.

photoinduced change in the absorbance coincide with those measured for *I* in the absence of benzophenone (Fig. 4). However, in the presence of benzophenone, the photoinduced absorption ( $\Delta A$ ) increases, indicating an efficient population of the triplet state of the dye molecule upon sensitized photoexcitation. It is known that the triplet-triplet absorption maximum of benzophenone is at 525 nm and the triplet lifetime is 50  $\mu$ s [16]. This means that the spectrum and the kinetics of the change in the absorbance shown in Fig. 6 are the consequences of sensitized population of the triplet level of molecule *I*.

Fig. 7 shows the kinetic curves for the change in absorbance measured upon laser excitation *I* at 480 nm and 680 nm in the absence (1) and in presence (2) of ascorbic acid. The decrease in the lifetime of the reaction intermediate in the presence of electron donor indicates that the intermediate is the cation radical of *I* ( $R^{\cdot+}$ ).

It is noteworthy that electron acceptors, methyl viologen and *para*-nitroacetophenone, had no effect on the kinetics of photoconversion of *I*. This may be attributable to the absorption of the anion radical ( $R^{\cdot-}$ ) in the short-wavelength spectral region, which hampered recording of the spectrum because of design features of the setup used for spectral kinetic measurements.

Kinetic measurements of the change in the photoinduced absorption on a microsecond time scale (insets of Fig. 5a and b) provided grounds for interpreting the short-lived intermediates at  $\lambda = 480$  nm as being due to superposition of T-T absorption and electron transfer processes. Presumably, the electron transfer yielding the radical species may occur as the reaction of dismutation of molecules in the triplet state [22].

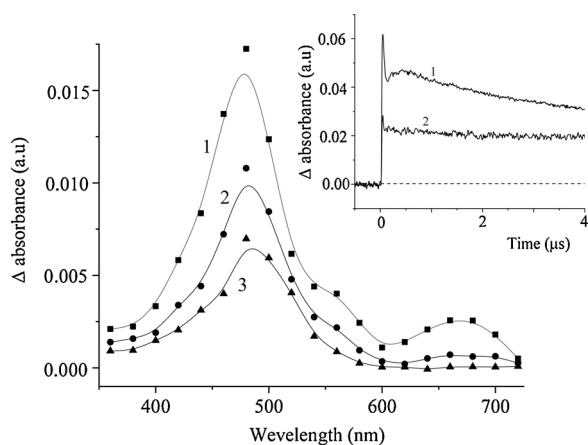


**Fig. 8.** Photoinduced absorption spectra of oxygen-free solution of *I* in the presence of  $\text{Pb}(\text{ClO}_4)_2$  measured at 2 (1), 75 (2), and 425 (3)  $\mu\text{s}$ . The inset shows the kinetic curves for the change in the photoinduced absorption of oxygen-free solutions at 480 nm in the absence (1) and in presence of  $\text{Pb}(\text{ClO}_4)_2$  (2). Concentrations: *I*,  $2 \times 10^{-5}$ ;  $\text{Pb}(\text{ClO}_4)_2$ ,  $2 \times 10^{-5}$  mol/L.

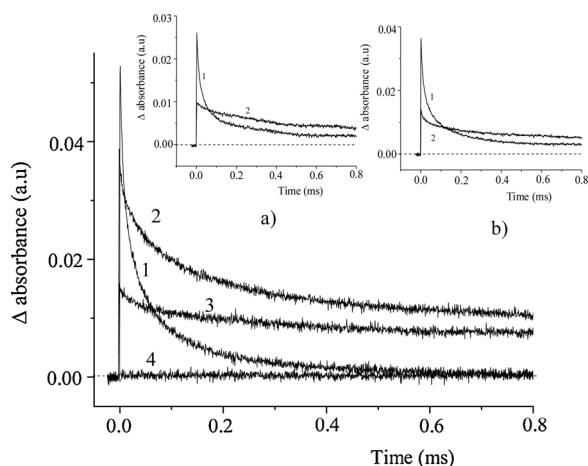
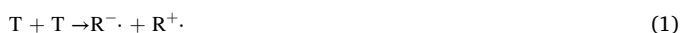


**Fig. 9.** Kinetic curves for the change in the photoinduced absorption of oxygen-free solutions of *I* in the absence (1) and in presence of  $\text{Pb}(\text{ClO}_4)_2$  in concentrations of  $1 \times 10^{-5}$  (2),  $2 \times 10^{-5}$  (3), and  $5 \times 10^{-5}$  (4) mol/L and  $\lambda = 480$  nm. The insets show the analogous kinetic curves measured in the absence (1) and in presence of  $\text{Ba}(\text{ClO}_4)_2$  (a) and  $\text{KClO}_4$  (b). Concentrations: *I*,  $2 \times 10^{-5}$ ;  $\text{Ba}(\text{ClO}_4)_2$ ,  $2 \times 10^{-5}$ ; and  $\text{KClO}_4$ ,  $2 \times 10^{-4}$  mol/L.



The absence of quenching of the short-lived product (triplet state) upon oxygen may be indicative of its short lifetime. Thus, apart from the triplet state of compound *I*, which is formed upon the laser pulse, a relatively long-lived intermediate is formed, as a cation radical.

Fig. 8 shows the difference spectra, and Fig. 9 and the inset of Fig. 8 present the corresponding kinetic curves for the photoinduced absorption of *I* measured in the presence of lead perchlorate. A difference spectrum of the same type is also observed for the complex  $I\text{-Ba}^{2+}$ .

The difference absorption spectrum virtually coincides with the corresponding spectrum recorded for the free dye. The kinetic curves were measured at the maxima of absorbance change at 680 nm (a) and 480 nm (b) at different concentrations of lead perchlorate. The insets show the kinetic curves for the change of the absorbance measured for the complexes  $I\text{-K}^+$  and  $I\text{-Ba}^{2+}$ .

The kinetics in the absorbance is biexponential, with rate constants depending on the metal cation concentration. The data are summarized

**Table 2**

The rate constant for the relaxation of reaction intermediates for oxygen-free solutions of *I* measured at 480 nm for different concentrations of  $\text{Pb}(\text{ClO}_4)_2$ .

Concentration $\text{Pb}(\text{ClO}_4)_2$	$k_1, \text{s}^{-1}$	$k_2, \text{s}^{-1}$
0	$6 \times 10^4$	$8 \times 10^3$
$1 \times 10^{-5}$	$3 \times 10^4$	$5 \times 10^3$
$2 \times 10^{-5}$	$4 \times 10^4$	$3 \times 10^3$

in Table 2.

The dependence of the rate constants on the metal cation concentration attests to a change in the composition of the complex. It can be expected that, by analogy with *II* [23], an increase of the metal cation concentration should be accompanied by dimerization of the 1:1 complex ( $I\text{-Pb}^{2+}$ ), yielding the bis-sandwich 2:2 complex ( $2I\text{-2Pb}^{2+}$ ). In the presence of high concentrations of lead perchlorate ( $\geq 5 \times 10^{-5}$  mol/L), the cyclobutane may be formed in the course of [2 + 2]-photocycloaddition [24,25].

In the case of bis(15-crown-5)-1,4-distyrylbenzene (*II*), three equilibria were detected in the presence of metal cations, depending on the metal cation concentration [23].



where  $L = II$

The kinetic curves of the change in the photoinduced absorption measured in the presence of  $\text{Ba}(\text{ClO}_4)_2$  virtually coincide with analogous curves measured in the presence of  $\text{Pb}(\text{ClO}_4)_2$ . In the presence of  $\text{KClO}_4$ , no cyclobutane formation was observed up to concentration of  $2 \times 10^{-4}$  mol/L.

The inset of Fig. 8 illustrates the effect of  $\text{Pb}^{2+}$  on the photo-conversion kinetics of short-lived photoreaction intermediates. The presence of  $\text{Pb}(\text{ClO}_4)_2$  decreases the rate of dismutation and the yield of radicals. A specific feature of the lead cation is that the complex formation of *I* with  $\text{Pb}(\text{ClO}_4)_2$  is expected to increase the probability of intersystem crossing and to decrease the triplet state lifetime due to the heavy atom effect, as has been observed for *II* [13]. This is indicated by a sharp drop of the fluorescence quantum yield in the presence of  $\text{Pb}(\text{ClO}_4)_2$  (Table 1). The absence of noticeable changes in the difference absorption spectra and in the relaxation times of intermediates measured in the absence and in presence of  $\text{Pb}(\text{ClO}_4)_2$  may be indicative of a short triplet state lifetime ( $< 2 \mu\text{s}$ ) and of the formation of radical species in the photoreaction.

### 3.3. Quantum chemical calculations

#### 3.3.1. Energy of trans-cis-isomerization

The optimized structure of dye *I* with atom numbering is depicted in Fig. 10.

The *cis*-isomers are formed upon internal rotation around the dihedral angles  $\chi_1$  (28-29-30-14 atoms) or  $\chi_2$  (17-16-15-12 atoms). In the ground state, both C=C double bonds formed by the  $\text{C}_{29}\text{-C}_{30}$  atoms and the  $\text{C}_{15}\text{-C}_{16}$  atoms occur in the *trans,trans*-configuration designated by  $I_{tt}$ . The calculations show that, except for the crown ether moieties, which have somewhat different dihedral angles, the molecule is nearly planar. Therefore, the electron density is delocalized over the whole  $\pi$ -system, with the difference that the  $\pi$ -system (unlike that of *II*) is not alternant, because of the *meta*-orientation of 15-crown-5-styryl moieties (see below). It can be seen in Fig. 10 that the bond lengths in the moieties are equal in pairs to the third decimal place.

The *trans-cis*-isomerization, which occurs via internal rotation around the C=C bonds upon photoexcitation, may give rise to four



**Table 5**Total energies,  $E_{\text{total}}$  (a.u.) and complex formation energies,  $\Delta E_{\text{comp}}$  (kcal/mol).

System, Calculation method	$S_0$	$\Delta E_{\text{comp}}$	$S_1$	$\Delta E_{\text{comp}}$
$I$ ( <i>ab initio</i> ) <sup>a</sup>	-2237.40717	-	-2237.30027	-
$I\text{-Ba}^{2+}$ (DFT) <sup>b</sup>	-2248.92381	-	-2248.91969	-
$2I\text{-}2\text{Ba}^{2+}$ (DFT) <sup>b</sup>	-4498.10816	-163.5	-4498.01455	-107.3
$I\text{-Ba}^{2+}$ ( <i>ab initio</i> ) <sup>b</sup>	-2239.86980	-	-2239.77393	-60.2 <sup>a</sup>
$2I\text{-}2\text{Ba}^{2+}$ ( <i>ab initio</i> ) <sup>c</sup>	-4479.86959	-81.6 /- 131.3 <sup>d</sup>	-4479.69201	-30.3 /- 80.5 <sup>d</sup>

<sup>a</sup> def2-SVP basis set.<sup>b</sup> Calculation with D3.<sup>c</sup> def2-TZVP basis set.<sup>d</sup>  $\Delta E_{\text{comp}}$  without D3/with D3.

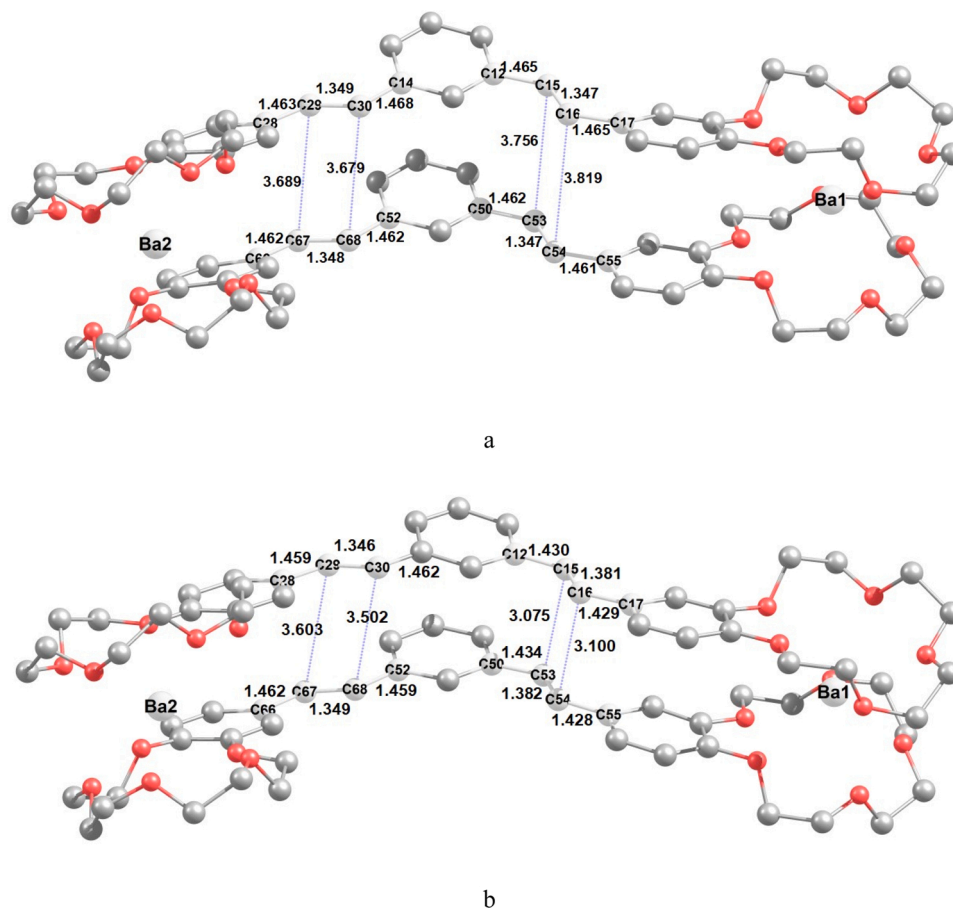
compound  $II$  forms *bis*-sandwich complexes  $2II\text{-}2\text{Ba}^{2+}$  [23], the same possibility cannot also be ruled out for  $I$  with the assumption that complex  $2I\text{-}2\text{Ba}^{2+}$  could subsequently be converted to a cyclobutane derivatives. Previously, the structures appearing in Eqs. 1–3 for  $II$  were calculated by the DFT methods [13]. In this study, the structures of  $I$  and its  $\text{Ba}^{2+}$  complexes were also calculated by DFT with full geometry optimization with the dispersion correction D3. For higher reliability, the wave functions and the formation energies of the *bis*-sandwich complex  $2I\text{-}2\text{Ba}^{2+}$  were calculated by the *ab initio* method. The goal of the quantum chemical study was to prove the possibility of formation of *bis*-sandwich complexes  $2I\text{-}2\text{Ba}^{2+}$ . The total energies of  $I$  and the complex formation energies of  $I$  with the barium cation are summarized in Table 5.

It follows from Table 5 that the complex  $2I\text{-}2\text{Ba}^{2+}$  can exist both in

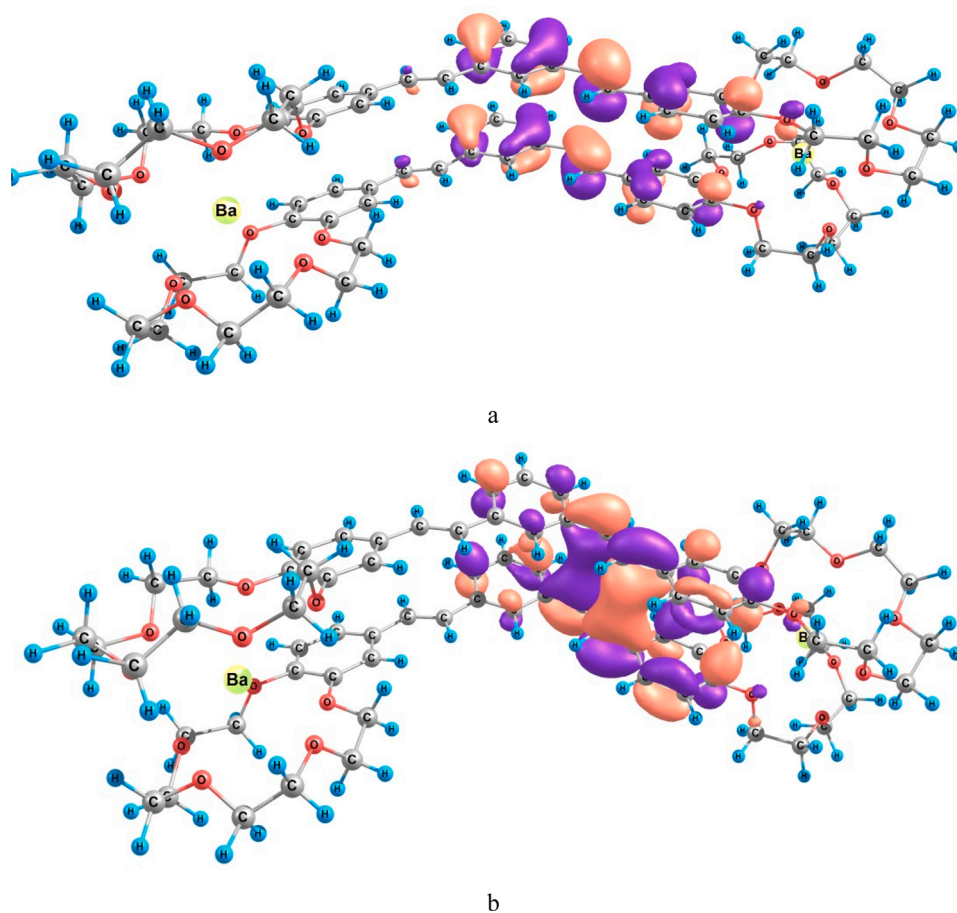
the ground  $S_0$  and excited  $S_1$  states. If the dispersion correction is taken into account,  $\Delta E_{\text{comp}}$  values in the DFT approximation are fairly high; however, this result cannot be verified experimentally. The *ab initio* calculation resulted in a lower  $\Delta E_{\text{comp}}$ . Comparison of the  $\Delta E_{\text{comp}}$  values calculated with D3 and without D3 demonstrates a large contribution of van der Waals interactions to the complex formation energy, which is not surprising, as both extended planar  $\pi$ -systems of  $I$  are held at a relatively short distance above one another by two barium cations, which provides for  $\pi$ -stacking interactions between the components. As can be seen from Table 5, the  $\Delta E_{\text{comp}}^*$  value in the  $S_1$  state is lower than  $\Delta E_{\text{comp}}$  in the ground state. The reason is that the excited state of  $2I\text{-}2\text{Ba}^{2+}$  is formed from a  $I(S_0)$  and  $I(S_1)$  pair and, since the energy level  $E_{\text{total}}I(S_0)$  is by definition lower than  $E_{\text{total}}I(S_1)$ , then  $E_{\text{total}}(2I\text{-}2\text{Ba}^{2+}) < E_{\text{total}}(2I\text{-}2\text{Ba}^{2+})$  in the absolute value. The calculated difference between these values is the excitation energy.

Fig. 11 shows the DFT/D3-optimized structures of  $2I\text{-}2\text{Ba}^{2+}$  in the ground  $S_0$  (a) and excited  $S_1$  (b) states.

The key difference between the structures is as follows. First, excitation of the complex is accompanied by a decrease in the interplanar spacing between the chromophores, moreover, the decrease is non-equivalent. Indeed, the right parts of the chromophores are located more closely to each other (the average length,  $l_{\text{av}}$  3.09 Å) than the left parts ( $l_{\text{av}}$  3.55 Å). The average lengths of the Ba-O coordination bonds virtually do not change ( $l_{\text{av}}$  2.8 Å). Second, the C=C distance and adjacent interatomic distances in the left part show more alternation than those in the right part. That is, alternation of double and single bond lengths is more clearly defined in the left part (1.46 – 1.348 – 1.461 Å) than in the right part (1.432 – 1.382 – 1.429 Å). This means that the electron density around the C=C bond and adjacent bonds is



**Fig. 11.** Structures of complexes  $2I\text{-}2\text{Ba}^{2+}$  in the ground  $S_0$  (a) and excited  $S_1$  (b) states calculated by DFT and TD DFT methods with the PBE0 functional in the SVP basis set.



**Fig. 12.** Structures of HOMO (a) and LUMO (b) of  $2I-2Ba^{2+}$  in the excited  $S_1$  state (b) calculated by *ab initio* method in the TZSVP three-exponential basis set. Different colors correspond to the phase of wave functions, their volumes being proportional to the degree of orbital interaction.

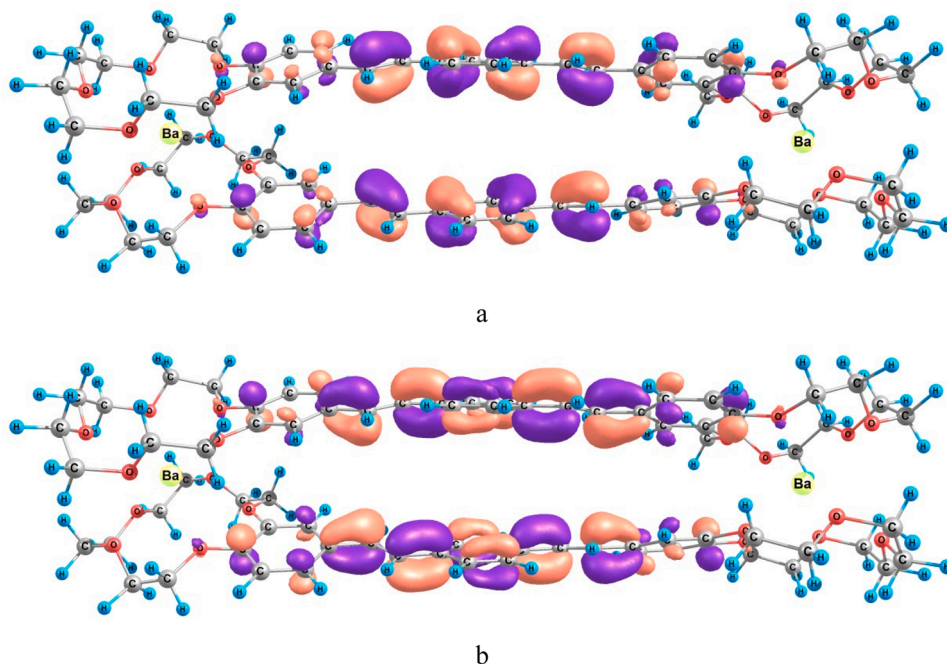


**Fig. 13.** Structures of HOMO (a) and LUMO (b) of  $2II-2Ba^{2+}$  in the excited  $S_1$  state (b) calculated by *ab initio* method in the TZSVP three-exponential basis set.

more delocalized in the right part of the molecule than in the left part, which is confirmed by the double bond orders (*bo*). Indeed, *bo* are 1.856 and 1.818  $\bar{e}$  for the left and right C=C bonds, respectively. Third, despite the fact that  $l_{av}$  of the Ba-O coordination bonds little change upon excitation:  $l_{av}$  2.826 and 2.857 Å, for  $S_0$  state, and  $l_{av}$  2.837 and 2.827 Å, for  $S_1$  state, correspondingly, the donor-acceptor characteristics of the complex change significantly. Thus, in the ground state, the positive charges on the left and right barium atoms were 0.784 and 0.818  $\bar{e}$ , whereas in the excited states they sharply increased to 1.339 and 1.328  $\bar{e}$ . If one recalls that the initial charge of the barium cation was +2, then the barium cations have accepted 1.216 and 1.182  $\bar{e}$  in the ground state of  $2I\cdot 2Ba^{2+}$  and markedly less, 0.661 and 0.672  $\bar{e}$ , in the excited state of the same complex. This is a result of the overall loss of electron density by the organic chromophore upon excitation, accompanied by electron transition from occupied to unoccupied levels.

The key feature of the electronic structure of the chromophore in *I* is that its  $\pi$ -system is not alternant, unlike that in *II* studied previously [13]. This is manifested as the absence of conjugation between the left and right parts of the chromophore; therefore, compounds *I* and *II* are expected to differ in reactivity. The information that bis-sandwich complexes  $2I\cdot 2Ba^{2+}$  can undergo photocycloaddition was derived from analysis of the structures of the highest occupied (HOMO) and lowest unoccupied (LUMO) orbitals, as excitation primarily affects the electron transition from the former to the latter. Fig. 12 shows the HOMO and LUMO structures for  $2I\cdot 2Ba^{2+}$  in the  $S_1$  state calculated by *ab initio* method in the three-exponential basis set.

The key role of  $Ba^{2+}$  cations in the complex is to hold both chromophores approximately parallel to each other as a sandwich and, as a result, the interplanar spacing does not exceed four angstroms. This gives rise to an orbital bonding between the chromophores, and the electron density is delocalized within the complex. In Fig. 12a, it can be seen that HOMO is an antibonding orbital between the upper and lower  $\pi$ -systems of the right halves of the complex; furthermore, the HOMO electron density is concentrated in the right part, which is due to the absence of conjugation between the left and right halves. In turn, LUMO is a bonding orbital embracing the upper and lower chromophores; as a result, a bonding area appears between the chromophores upon photo-excitation accompanied by electron transition to the LUMO. This attests to a clear tendency towards chemical bond formation between the pair of upper and lower carbon atoms (belonging to the upper and lower double bonds), leading to the formation of cyclobutane derivative.

Unlike  $2I\cdot 2Ba^{2+}$ , in which the electron density is arranged asymmetrically because of the non-alternant character of the  $\pi$ -system,  $2II\cdot 2Ba^{2+}$  is an alternant system with fully delocalized electron density distribution along each of the chromophores and with orbital bond between the planes. The HOMO and LUMO of  $2II\cdot 2Ba^{2+}$  in the excited  $S_1$  state are shown in Fig. 13.

It can be seen that unlike that in  $2I\cdot 2Ba^{2+}$ , the HOMO electron density in  $2II\cdot 2Ba^{2+}$  is fully delocalized along the  $\pi$ -systems of both chromophores constituting the complex and is simultaneously an antibonding orbital between the upper and lower  $\pi$ -systems. In turn, LUMO is a bonding orbital between the upper and lower  $\pi$ -systems, although the degree of bonding is lower than in the case of LUMO of  $2I\cdot 2Ba^{2+}$ , because of the greater electron density delocalization along the overall  $\pi$ -system of the complex. This means that the trend towards formation of the cyclobutane derivative can also be followed for  $2II\cdot 2Ba^{2+}$ , but probably it has a lower probability than in  $2I\cdot 2Ba^{2+}$  due to higher electron density concentration in one half of the complex.

#### 4. Conclusions

The triplet state was found to involve in the photoconversion of *bis* (15-crown-5)-1,3-distyrylbenzene. The T-T dismutation, resulting in the formation of radical products of the photoreaction ( $R^{\cdot-} + R^{\cdot+}$ ), was proposed to occur apart from T-T absorption to explain the kinetics of variation of the photoinduced absorption. The use of ascorbic acid as an

electron donor decreases the lifetime of the cation radical. The presence of  $Pb^{2+}$  decreases the T-T dismutation of triplet molecules and, hence, the yield of radicals. In the presence of  $Pb^{2+}$  or  $Ba^{2+}$ , the formation of complexes  $2I\cdot 2M^{2+}$  is probably accompanied by [2 + 2]-cycloaddition reaction.

Quantum chemical calculations indicate the formation of *bis*-sandwich complexes  $2I\cdot 2Ba^{2+}$  and their higher proneness to photocycloaddition in comparison with the analogous *bis*-sandwich complexes  $2II\cdot 2Ba^{2+}$ . This difference is due to the fact that the chromophore in *I* is not alternant and, hence, the electron density in  $2I\cdot 2Ba^{2+}$  is concentrated in one half of the molecule, thus resulting in a higher interplanar charge density in the excited state. This corresponds to higher probability of photocycloaddition, which binds the upper and lower chromophore to give a cyclobutane derivative. In turn, the chromophore  $\pi$ -system in *II* is alternant and, hence, the electron density is fully delocalized along the chromophores and, consequently, the interplanar charge is less concentrated, which decreases the photocycloaddition probability.

The results of this work can be used for the targeted design of photoactive supramolecular assemblies and for the development of optical molecular sensors based on distyrylbenzenes.

#### Author statement

The authors are grateful to the reviewers for their comments. The authors responded in detail to the comments made and made the appropriate changes to the text of the manuscript. The authors hope that the esteemed editor will consider our answers and changes made to the text of the article sufficient for the manuscript to be published in the journal.

#### Declaration of Competing Interest

The authors state that the publication of this article does not imply any conflict of interest.

#### Acknowledgments

This study was supported by the Russian Science Foundation (Project No. 19-13-00020) as related to the photonics of distyrylbenzene and its complexes and by the Ministry of Science and Higher Education within the state assignment for the Federal Scientific Research Center "Crystallography and Photonics", Russian Academy of Sciences, as related to the synthesis of distyrylbenzene and quantum chemical calculations of the structures of compounds in different states.

#### Appendix A. Supplementary data

Supplementary material related to this article can be found, in the online version, at doi:<https://doi.org/10.1016/j.jphotochem.2021.113293>.

#### References

- [1] S.P. Gromov, Molecular mecano for light-sensitive and light-emitting nanosized systems based on unsaturated and macrocyclic compounds, Russ. Chem. Bull. 57 (2008) 1325–1350, <https://doi.org/10.1007/s11172-008-0174-9>.
- [2] S.Z. Vatsadze, S.P. Gromov, Novel linear bis-crown receptors with cross-conjugated and conjugated central cores, Macroheterocycles 10 (2017) 432–445, <https://doi.org/10.6060/mhc171142v>.
- [3] D. Oelkrug, A. Tompert, H.J. Egelhaaf, M. Hanack, E. Steinhuber, M. Hohloch, H. Meier, U. Stalmach, Towards highly luminescent phenylene vinylene films, Synth. Met. 83 (1996) 231–237, [https://doi.org/10.1016/s0379-6779\(96\)04484-0](https://doi.org/10.1016/s0379-6779(96)04484-0).
- [4] B.J. Laughlin, T.L. Duniho, S.J. El Homsy, B.E. Levy, N. Deligonul, J.R. Gaffen, J. D. Protasiewicz, A.G. Tennyson, R.C. Smith, Comparison of 1,4-distyrylfluorene and 1,4-distyrylbenzene analogues: synthesis, structure, electrochemistry and photophysics, Org. Biomol. Chem. 11 (2013) 5425, <https://doi.org/10.1039/c3ob40580j>.

- [5] K. Sandros, M. Sundahl, O. Wennerstru, U. Norinder, Cis-trans photoisomerization of a p-styrylstilbene, a one- and twofold adiabatic process, *J. Am. Chem. Soc.* 112 (1990) 3082–3086, <https://doi.org/10.1021/ja00164a031>.
- [6] E. Marri, F. Elisei, U. Mazzucato, D. Pannacci, A. Spalletti, Triplet-sensitized photobehaviour of the three stereoisomers of 1,4-distyrylbenzene and some aza-analogues, *J. Photochem. Photobiol. A* 177 (2006) 307–313, <https://doi.org/10.1016/j.jphotochem.2005.06.010>.
- [7] M. Kim, D.R. Whang, J. Gierschner, S.Y. Park, A distyrylbenzene based highly efficient deep red/near-infrared emitting organic solid, *J. Mater. Chem. C* 3 (2015) 231–234, <https://doi.org/10.1039/c4tc01763>.
- [8] M. Cavazzini, S. Quici, S. Orlandi, C. Sissa, F. Terenziani, A. Painelli, Intimately bound coumarin and bis(alkylaminostyryl)benzene fragments: synthesis and energy transfer, *Tetrahedron* 69 (2013) 2827–2833, <https://doi.org/10.1016/j.tet.2013.01.075>.
- [9] A. Chaieb, A. Khoukh, R. Brown, J. Francois, C. Dagron-Lartigau, Characterization of model luminescent PPV analogues with donating or withdrawing groups, *Opt. Mater.* 30 (2007) 318–327, <https://doi.org/10.1016/j.optmat.2006.11.052>.
- [10] B.S. Kalanoor, P.B. Bisht, S. Annamalai, I.S. Aidhen, A new distyrylbenzene derivative with Weinreb amide functionality: an efficient laser dye and nonlinear optical material, *J. Lumin.* 129 (2009) 1094–1098, <https://doi.org/10.1016/j.jlumin.2009.05.003>.
- [11] J. Motoyoshiya, Z. Fengqiang, Y. Nishii, H. Aoyama, Fluorescence quenching of versatile fluorescent probes based on strongly electron-donating distyrylbenzenes responsive to aromatic chlorinated and nitro compounds, boronic acid and  $\text{Ca}^{2+}$ , *Spectrochim. Acta A* 69 (2008) 167–173, <https://doi.org/10.1016/j.saa.2007.03.024>.
- [12] S.J.K. Pond, O. Tsutsumi, M. Rumi, O. Kwon, E. Zojer, J.L. Bredas, S.R. Marder, J. W. Perry, Metal-ion sensing fluorophores with large two-photon absorption cross sections: aza-crown ether substituted donor–Acceptor–Donor distyrylbenzenes, *J. Am. Chem. Soc.* 126 (2004) 9291–9306, <https://doi.org/10.1021/ja049013t>.
- [13] L.S. Atabekyan, V.G. Avakyan, A.K. Chibisov, S.P. Gromov, S.Z. Vatsadze, V. N. Nuriev, A.V. Medved'ko, Bis(15-crown-5)-1,4-distyrylbenzene and its complexes with metal perchlorates: photonic and structure, *Russ. Chem. Bull.* 11 (2019) 2053–2064, <https://doi.org/10.1007/s11172-019-2666-1>.
- [14] V.N. Nuriev, O.V. Fedorov, A.A. Moiseeva, A.Ya. Freidzon, N.A. Kurchavov, Synthesis, structure, spectral properties, and electrochemistry of bis(crown ether) containing 1,3-distyrylbenzenes, *Russ. J. Org. Chem.* 53 (2017) 1726–1737, <https://doi.org/10.1134/s1070428017110203>.
- [15] L.S. Atabekyan, A.K. Chibisov, M.V. Alfimov, Pulse photolysis of crown ether styryl dyes and their complexes with metal ions, *High Energy Chem.* 31 (1997) 344–348.
- [16] M. Montalti, A. Kpedi, L. Prodi, M.T. Gandolfi, *Handbook of Photochemistry* (third edition), Taylor and Francis, London, 2006, p. 574.
- [17] D.N. Laikov, Fast evaluation of the electron density in auxiliary basis sets, *Chem. Phys. Lett.* 28 (1997) 151–156, [https://doi.org/10.1016/s0009-2614\(97\)01206-2](https://doi.org/10.1016/s0009-2614(97)01206-2).
- [18] D.N. Laikov, Y.A. Ustynyuk, PRIRODA-04: a quantum-chemical program suite. New possibilities in the study of molecular systems with the application of parallel computing, *Russ. Chem. Bull.* 54 (2005) 820–826, <https://doi.org/10.1007/s11172-005-0329-x>.
- [19] M. Kaupp, P.V.R. Schleyer, H. Stoll, H. Preuss, Pseudopotential approaches to Ca, Sr, and Ba hydrides. Why are some alkaline earth MX<sub>2</sub> compounds bent? *J. Chem. Phys.* 94 (1991) 1360–1366, <https://doi.org/10.1063/1.459993>.
- [20] F. Weigend, R. Ahlrichs, Balanced basis sets of split valence, triple zeta valence and quadruple zeta valence quality for H to Rn: design and assessment of accuracy, *Phys. Chem. Chem. Phys.* 7 (2005) 3297–3305, <https://doi.org/10.1039/b508541a>.
- [21] A.Ya. Freidzon, A.A. Safonov, A.A. Bagaturyants, M.V. Alfimov, Solvatofluorochromism and twisted intramolecular charge-transfer state of the Nile red DyeInt, *Int. J. Quantum Chem.* V.112 (2012) 3059–3067, <https://doi.org/10.1002/qua.24233>.
- [22] V.E. Korobov, A.K. Chibisov, Primary photoprocesses in colorant molecules, *Russ. Chem. Rev.* 52 (1983) 27–42, <https://doi.org/10.1070/rc1983v052n01abeh002795>.
- [23] A.I. Vedernikov, V.N. Nuriev, O.V. Fedorov, A.A. Moiseeva, N.A. Kurchavov, L. G. Kuz'mina, A.Ya. Freidzon, E.S. Pod'yacheva, A.V. Medved'ko, S.Z. Vatsadze, S. P. Gromov, Synthesis, structure and complexation of biscrown-containing 1,4-distyrylbenzenes, *Russ. Chem. Bull.* 65 (2016) 2686–2703, <https://doi.org/10.1007/s11172-016-1637-z>.
- [24] S.P. Gromov, O.A. Fedorova, E.N. Ushakov, A.V. Buevich, I.I. Baskin, Y.V. Pershina, B. Eliasson, U. Edlund, M.V. Alfimov, Photoswitchable molecular pincers: synthesis, self-assembly into sandwich complexes and ion-selective intramolecular [2 + 2]-photocycloaddition of an unsaturated bis-15-crown-5 ether, *J. Chem. Soc. Perkin Trans. 2* (1999) 1323–1330, <https://doi.org/10.1039/a902151e>.
- [25] S.P. Gromov, A.I. Vedernikov, N.A. Lobova, L.G. Kuz'mina, S.S. Basok, Y. A. Strelenko, M.V. Alfimov, J.A.K. Howard, Controlled self-assembly of bis(crown) stilbenes into unusual bis-sandwich complexes: structure and stereoselective [2 + 2] photocycloaddition, *New J. Chem.* 35 (2011) 724–737, <https://doi.org/10.1039/c0nj00780c>.